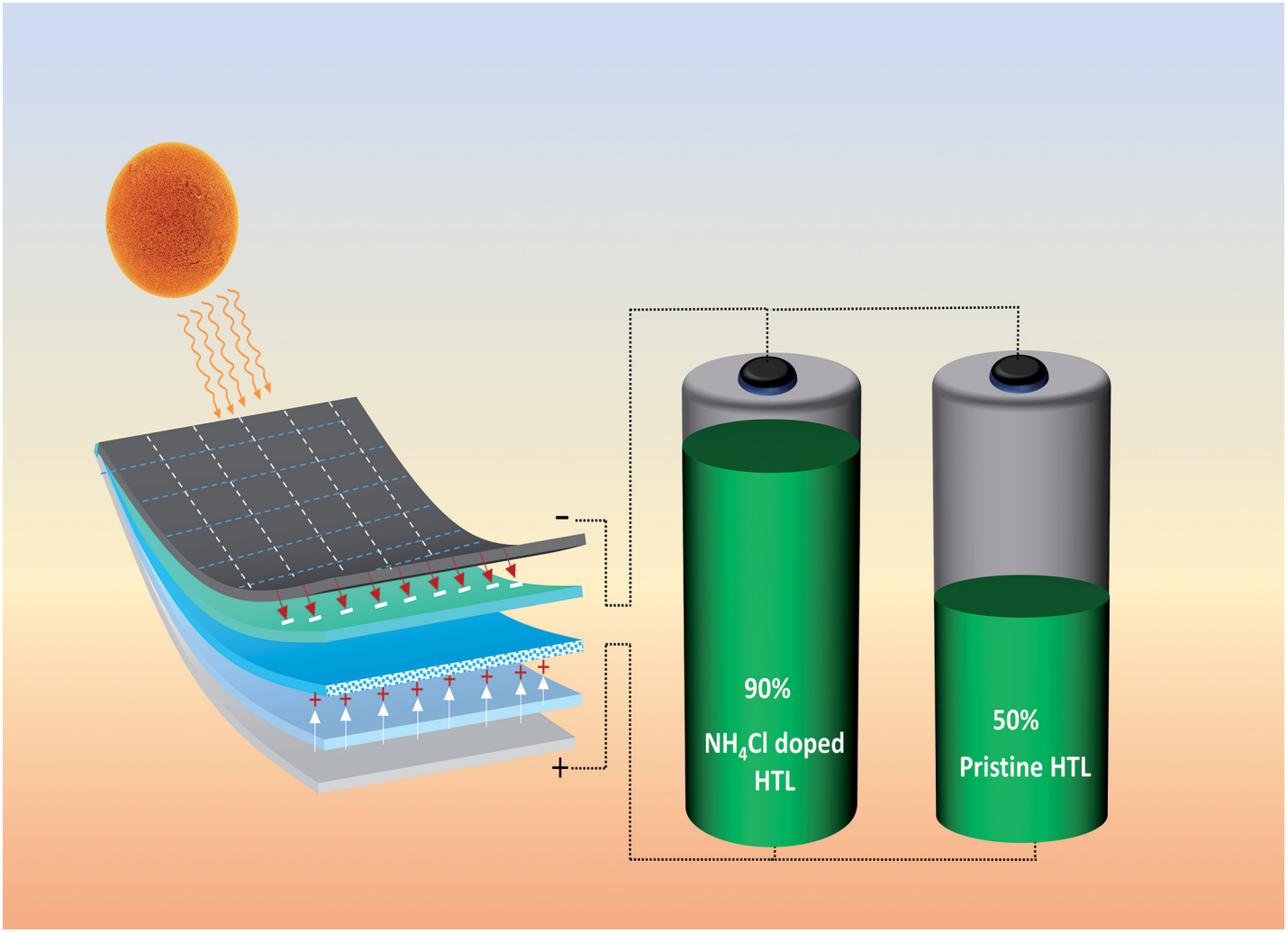

Showcasing research work by Shahid Zaman *et al.* from Department of Mechanical and Energy Engineering, Southern University of Science and Technology, Shenzhen China

Harnessing solar energy with NH_4Cl-doped hole transport layers in inverted perovskite solar cells

This work highlights the improved performance of hole transfer layer achieved by optimized NH_4Cl doped PEDOT: PSS towards a superior power conversion efficiency.

As featured in:

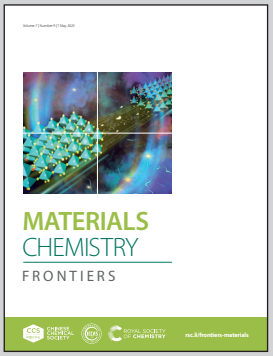

See Shahid Zaman *et al.*, *Mater. Chem. Front.*, 2023, **7**, 1813.

Registered charity number: 207890

MATERIALS CHEMISTRY
FRONTIERS

RESEARCH ARTICLE

View Article Online
View Journal | View Issue

Cite this: *Mater. Chem. Front.*, 2023, **7**, 1813

Harnessing solar energy with NH_4Cl-doped hole transport layers in inverted perovskite solar cells†

Sikandar Iqbal,[a] Aadil Nabi Chishti,[a] Muhammad Bilal Hussain,[b] Fakhr uz Zaman,[b] Abdul Qayum,[a] Rashid Mehmood[d] and Shahid Zaman*[c]

Inverted perovskite solar cells have received enormous attention due to exceptional photovoltaic performance, yet they are susceptible to hysteresis and low conductivity. Poly 3,4-ethylenedioxythiophene: Poly 4-styrenesulfonate (PEDOT: PSS) is a widely utilized material in inverted perovskite solar cells as hole transporting layers. However, the low conductivity of the PEDOT: PSS is a significant hurdle toward high power conversion efficiency. Herein, we report an efficient and straightforward approach to modify the intrinsic properties of PEDOT: PSS *via* doping various amounts of ammonium chloride (NH_4Cl). Systematic observations have explored a significant transformation in the intrinsic properties of NH_4Cl doped PEDOT: PSS, resulting in higher conductivity compared with pristine PEDOT: PSS. The optimized NH_4Cl doped PEDOT: PSS exhibits higher surface roughness which not only improves the contact area between the active layer and the anode layer but also enhances the spectral absorption with a subsequent increase in the light-harvesting ability. As a result, the optimized NH_4Cl doped PEDOT: PSS delivers a superior power conversion efficiency (PCE), an open circuit voltage (V_{OC}), a short circuit current density (J_{SC}), and a fill factor (FF) of 17.5%, 1.02 V, 26.4 mA cm^{-1} and 79.7%, respectively. We believe that this study will offer profound insights into the efficient and cost-effective synthesis of high-power conversion efficiency inverted perovskite solar cells.

Received 4th January 2023,
Accepted 15th March 2023

DOI: 10.1039/d3qm00012e

rsc.li/frontiers-materials

The current sources of energy predominantly rely on non-renewable fossil fuels such as coal, oil, and natural gas. However, the escalating usage of these finite resources has raised concerns about their sustainability and environmental impact.[1–4] The challenge of meeting energy demands has been addressed through the development of advanced photovoltaic technologies and the use of perovskite solar cells (PSCs) to efficiently produce solar energy.[5–7] Organic–inorganic hybrid PSCs are one of the promising candidates for light harvesting and show great potential in energy storage devices due to their steady state and large absorption visible spectrum, high charge diffusion length and solution processability.[8,9] Multiple fabrication methods have been reported to establish the surface defective passivation and surface roughness. For instance, the post-solvent annealing growth, uniform grain boundaries, crystal growth and additive construction are among the most frequently used approaches.[10,11] The PCE is directly influenced by surface coverage, grain size distribution, and active layer film morphology.[12–14] Furthermore, the non-radiative charge recombination and passivation defect approaches may increase critical parameters such as open circuit voltage, fill factor, and hysteresis potentially improving the performance of PSCs.[15]

The hole transporting layer (HTL) is one of the best layers to accelerate the performance of PSCs in n-i-p type architecture between the light absorbing layer and the anode layer.[16] The modified HTL based devices can minimize the charge recombination, improving the transportation of holes and reducing the charge recombination.[17] In inverted PSCs, the HTL surface roughness and surface morphology have a significant influence on the crystal orientation of the perovskite layer and the PCE of the device.[18–23] Recently, superior performance has been achieved using several organic and inorganic HTL materials, such as PEDOT: PSS,[24] PTAA,[25] NiO_x,[26] CuI,[27] and CuO_x[28] employed in the inverted PSCs. However, due to the acidity of PEDOT: PSS, several undesirable problems resulted in low work function, which reduces the open circuit voltage and corrosion of the FTO electrode and diminishes the performance of the PSCs device. In addition, the core–shell behavior of PEDOT: PSS has relatively low conductivity compared with pristine PEDOT,

[a] *ZJU-Hangzhou Global Technological and Innovation Center, Zhejiang University, Hangzhou, 310027, China*
[b] *School of Energy and Power Engineering, Shandong University, Jinan, 250061, China*
[c] *Key Laboratory of Energy Conversion and Storage Technologies, Department of Mechanical and Energy Engineering, Southern University of Science and Technology, Shenzhen, 518055, China. E-mail: shahid@sustech.edu.cn*
[d] *University of Chinese Academy of Sciences, Beijing, 100049, China*

† Electronic supplementary information (ESI) available: Detailed experimental processes, characterization results, and additional electrochemical measurements. See DOI: https://doi.org/10.1039/d3qm00012e

which severely affects the PSCs performance.[29] Therefore, various techniques have been reported to enhance the intrinsic conductivity of PEDOT: PSS by incorporating several inorganic and organic hybrid compounds as dopants or additives, including sodium chloride,[30] lithium chloride,[31] ammonia,[32] Nafion,[33] silver nanoparticles,[34] gold silver core–shell,[35] and graphene oxide.[36] Similarly, some secondary dopants such as dimethyl sulfoxide, dimethylformamide, sorbitol and ethylene glycol are also employed.[37,38]

Herein, we have adopted a facile method to introduce NH_4Cl into the PEDOT: PSS solution, which was used as the HTL in the PSCs device. The optimized device configuration has resulted in higher optical, electrical, and chemical properties of the modified layer. We have investigated the drastic enhancement in conductivity of the HTL after being doped with NH_4Cl. The PSS serves as an insulating layer on the surface of the PEDOT conducting shell. The newly formed bond PSS-NH_4^+ might decrease the force of attraction between PEDOT and PSS, implying that the PSS layer becomes free and less coiled. At the same time, the PEDOT exhibits excellent charge transportation capability. The optimized NH_4Cl doped PEDOT: PSS layer leads to more hole extraction and ultimately enhances the photovoltaic properties of the champion PSCs device. As a result, the optimized NH_4Cl doped PEDOT: PSS delivers a superior PCE, V_{OC}, J_{SC}, and a FF of 17.5%, 1.02 V, 26.4 mA cm^{-2} and 79.7%, respectively.

Both organic and inorganic PSCs depend on the electrical conductivity of the HTL for hole extraction and propagation of ionic paths. From previous literature, it is reported that the electrical conductivity of the HTL (PEDOT: PSS) can be influenced by insulating PSSH, which may consequently suffer the PCE. In this work, the conductivity of the HTL is enhanced significantly by doping NH_4Cl into the PEDOT: PSS layer and tested through four points probe instrument. The detailed conductivity, roughness, and sheet resistance of pristine PEDOT: PSS and NH_4Cl doped PEDOT: PSS with various concentrations of NH_4Cl are displayed in Table S1 (ESI†). The amount of NH_4Cl is represented by NH-*x*, (where *x* represents concentrations in mg mL^{-1}). Generally, in conductive polymers like PEDOT: PSS, the conductivity arises from the conjugated polymer chains that allow efficient transport of charge carriers. NH_4Cl doping introduces positively charged impurities into the material, which act as additional charge carriers. At low dopant concentrations such as 2, 5 and 10 mg, the concentration of charge carriers increased and the materials become more conductive. However, as the concentration of the dopant is increased beyond 10 mg, the material becomes more heavily doped, and the concentration of charge carriers becomes more uniform. This is because the charge carriers are less able to transfer their charge to neighboring sites, reducing the overall conductivity of the material. Furthermore, the introduction of large amounts of positive charge can disrupt the conjugated polymer chains, reducing their ability to efficiently transport charge carriers and behave as a semiconductor. The as optimized NH_4Cl-10 doped base HTL shows higher conductivity (1.39×10^{-3}) than pristine PEDOT: PSS (5.3×10^{-4}). The increased conductivity of the film is due to the phase separation between PEDOT and PSS caused by the incorporation of NH_4Cl, which resulted in attraction towards PEDOT: PSS. Fig. 1a depicts the chemical structure of PEDOT: PSS, where

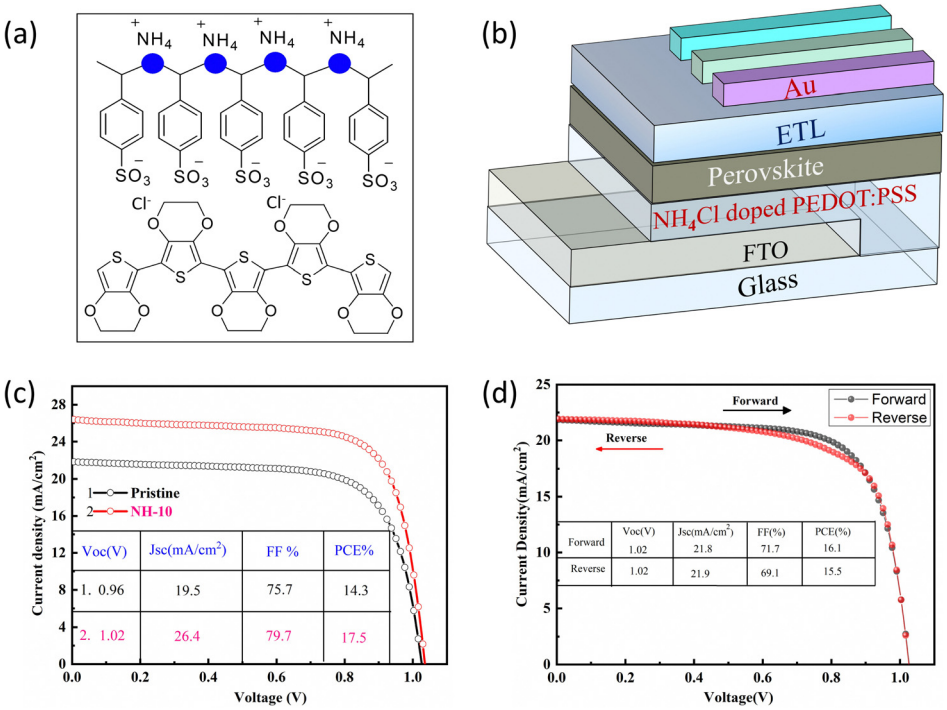

Fig. 1 (a) Chemical structure of PEDOT: PSS, (b) schematics diagram of PSCs, (c) typical *J*–*V* curves of the PSCs based pristine and NH_4Cl-10 doped PEDOT: PSS, (d) reverse and Forward scan of the NH_4Cl-10 doped PEDOT: PSS-based PSCs.

PSS serves as a non-conducting layer core on the surface of the conducting PEDOT shell. The NH_4Cl doped PEDOT: PSS decreased the force of attraction between PEDOT and PSS, resulting in the formation of new bonds between PSS-NH_4^+ as a result, the PSS shows more free movement and becomes less coiled. It is worth noting that the NH_4Cl doped PEDOT: PSS (HTL) exhibits stronger charge transportation capability and may achieve more hole extraction while remaining unchanged when impurities are added.[39]

The schematic diagram of PSCs shows the different layers drifted into the systematic design of FTO/PEDOT: PSS/or NH_4Cl-PEDOT: PSS/$MAPbI_{3-x}AC_2$/PCBM/BCP/Ag (Fig. 1b). The modified NH_4Cl-PEDOT: PSS layer base device exhibits the best performance compared with pristine PEDOT: PSS under the simulated solar radiation (AM 1.5G, 100 m W cm^{-2}) (Fig. 1c). The optimized device enhanced the FF value which might decrease the layer resistance and improve the conductivity of the HTL. The superior performance of the doped PEDOT: PSS base PSCs has significantly enhanced photovoltaic properties with the PCE, V_{OC}, J_{SC}, and FF of 17.5%, 1.02 V, 26.4 mA cm^{-2} and 79.7%, respectively. In contrast, the pristine PEDOT: PSS base PSCs have obtained PCE, V_{OC}, J_{SC}, and FF of 14.3, 0.96 V, 19.5 mA cm^{-2}, and 75.7%, respectively. It is speculated that the increased value of J_{SC} might be linked to the enhanced light-scattering, which decrease the reflection of light and ultimately absorb more photons. These photons further reduce the contact layer resistance and consequently improve the conductivity of PSCs.[40] In addition, when the concentration goes beyond 10 mg mL^{-1} (NH_4Cl-10), the photovoltaic performance decreases, even at a high dopant concentration of 50 mg mL^{-1} (NH_4Cl-50), a PCE value of 10.2% is achieved (Fig. S1 ESI†). The higher uniformity leads to a larger distance between the charge carriers, reducing the overall conductivity of the material, as the charge carriers become less efficient in transferring their charge to neighboring sites. It is worth noting that the modified base with an optimized concentration of the (NH-10) HTL shows excellent reverse and forward scans, achieving less hysteresis, signifying efficient PCE (Fig. 1d). The inferior photovoltaic performance at high concentrations shows that the HTL is insulating due to the large concentration of NH_4Cl, which hinders charge movement.

Furthermore, the optimized inverted PSCs have a high J_{SC} value compared with pristine PSCs, which is also verified through the external quantum efficiency (EQE) characterization tool ascribed to high surface roughness and a high degree of transmittance (Fig. 2a and Fig. S2 ESI†). The PCE of 45 devices from nine batches exhibits an average value of 16%, while 92% of the devices show a PCE value over 14%, with the highest value reported being 17.5% for three devices (Fig. 2b). Meanwhile, both the pristine and NH_4Cl doped PEDOT: PSS PSCs absorption spectra were virtually produced in the same ultraviolet region of 400–800 nm, indicating that the perovskite layer with NH_4Cl doped shows higher photon absorption capacity than pristine (Fig. 2c and Fig. S3 ESI†). It is worth noting that a solar cell with higher ultraviolet (UV) absorption can convert more photons into electricity, resulting in higher efficiency. Moreover, UV light can also contribute to more efficient charge

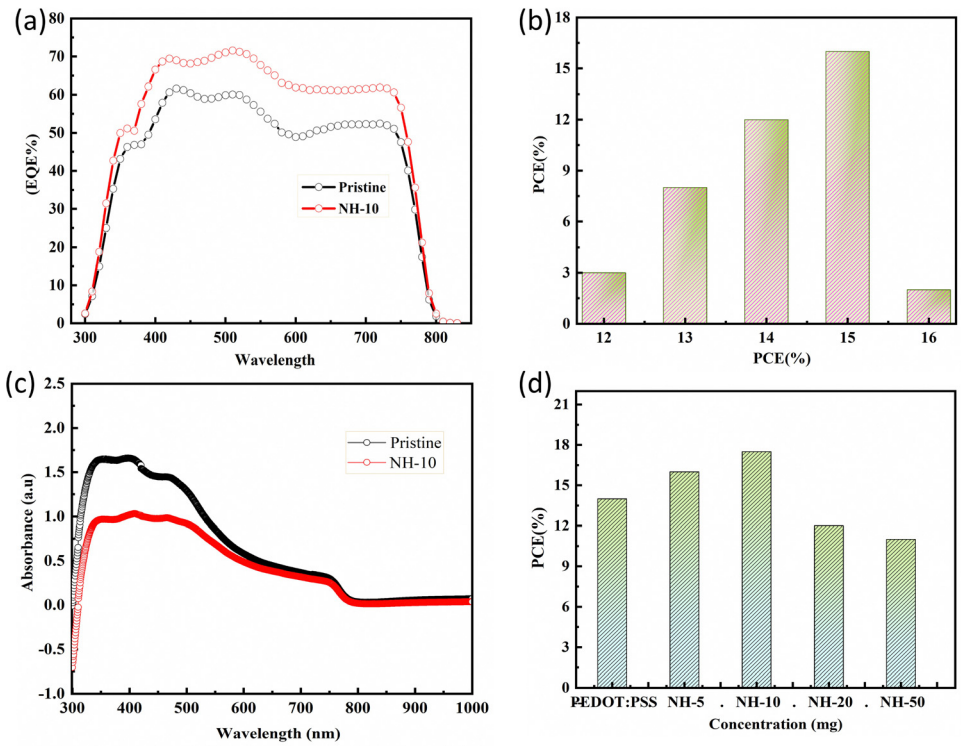

Fig. 2 Optoelectronic properties analysis (a) EQE spectra, (b) show the average value of PCE, and (c) UV-visible absorbance spectra for both pristine and NH_4Cl-10 doped PEDOT: PSS. (d) PEC of different doping concentrations.

separation and transport within the solar cell, leading to higher open-circuit voltage and fill factor, which also contributes to the overall photovoltaic performance. Additionally, Fig. 2d displays the power conversion efficiency *versus* various doping concentrations.

Atomic force microscopy (AFM) was implied to investigate the surface morphology of various doped concentrations of NH_4Cl on the surface of PEDOT: PSS (HTL). The surface of pristine PEDOT: PSS is quite smooth compared to doped PEDOT: PSS (Fig. S4 and S5 ESI†). The pristine PEDOT: PSS shows surface roughness with a root mean square (RMS) of 7.98 nm, which significantly increases to 15 nm after doping with 10 mg mL^{-1} NH_4Cl into PEDOT: PSS (Fig. 3a and b). It is vital to observe as the increases in surface roughness of the HTL could potentially increase the grain size after incorporating NH_4Cl. In addition, the group VII elements (especially chlorine Cl) imply that complexes obtained in the inorganic layer work as p-type dopants with unknown defects.[40] Cl shows the same homogenous impact in NH_4Cl when doped with the organic polymer layer PEDOT: PSS. Furthermore, the rougher surface may also improve the contact area between the active layer and the anode layer, enhancing spectral absorption by minimizing the reflection, which leads to enhanced light harvesting.[41] However, increasing concentration from 10 to 20, and 50 mg mL^{-1} raise the sheet resistance and have a detrimental influence on the surface of the HTL film, resulting in poor conductivity of highly concentrated PEDOT: PSS (Table S1 ESI†).

The surface morphologies and crystallization of the perovskite film on the surface PEDOT: PSS were further studied *via* scanning electron microscopy (SEM). The pristine PEDOT: PSS exhibits smooth surface morphology, while the NH_4Cl doped PEDOT: PSS shows high crystallinity, verified by the bright spots on the surface of the modified HTL (Fig. 3c and d, Fig. S6 ESI†). Due to surface roughness, the NH_4Cl doped PEDOT: PSS resulted in high photovoltaic performance. The detailed photovoltaic performance of the various doped NH_4Cl doped PEDOT: PSS is displayed in Table S2 (ESI†). Moreover, it is found that crystal growth increases the particle size, which plays a crucial role in separating the core and shell structure of the PEDOT: PSS. Meanwhile, increasing surface roughness decreases the sheet resistance which is favorable for charge carrier transportation and high hole generation.

Electrochemical impedance spectroscopy (EIS) is a non-destructive electrical characterization technique that measures the impedance of a solar cell over a range of frequencies. The impedance of a solar cell can be expressed as a combination of resistance and capacitance, which define the electrical properties of the cell. In the case of a solar cell with an increase in the Jsc value, EIS can provide further insight into the changes in the electrical properties of the cell that are responsible for the increased current. For instance, if the increase in the Jsc value is due to improved hole transport, EIS can provide evidence of changes in the electrical conductivity or recombination resistance of the hole-transport layer. This can be seen as changes in the impedance spectrum, such as a shift in the position of the

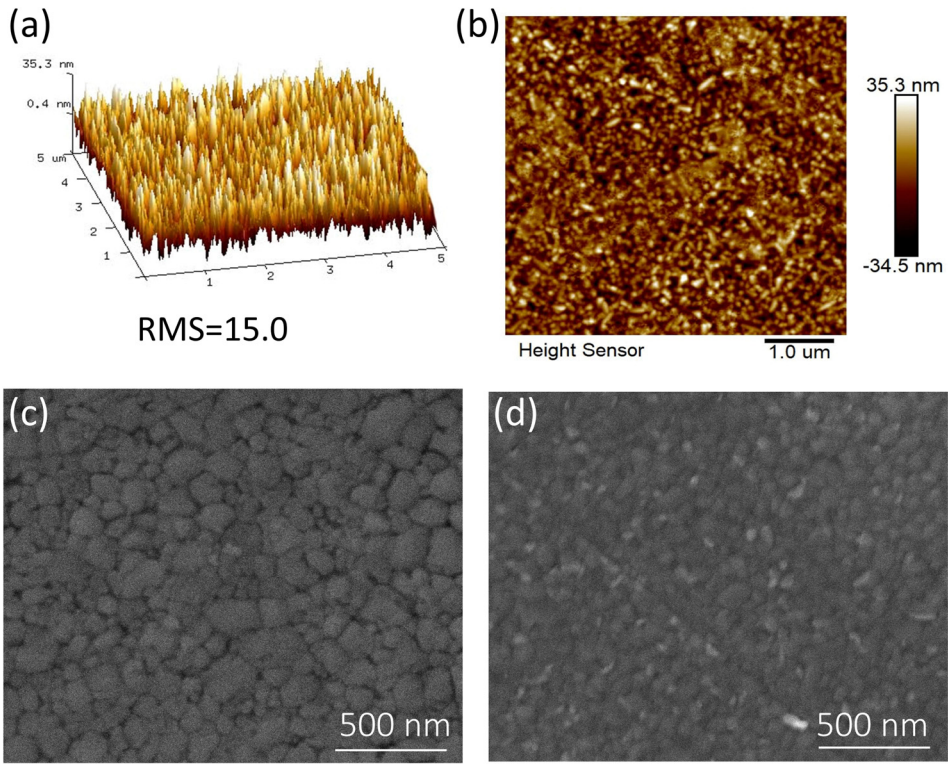

Fig. 3 Surface morphology analysis. (a and b) AFM topography of NH_4Cl-10 doped PEDOT: PSS, SEM images of perovskite films, (c) pristine, (d) NH_4Cl-10 PEDOT: PSS.

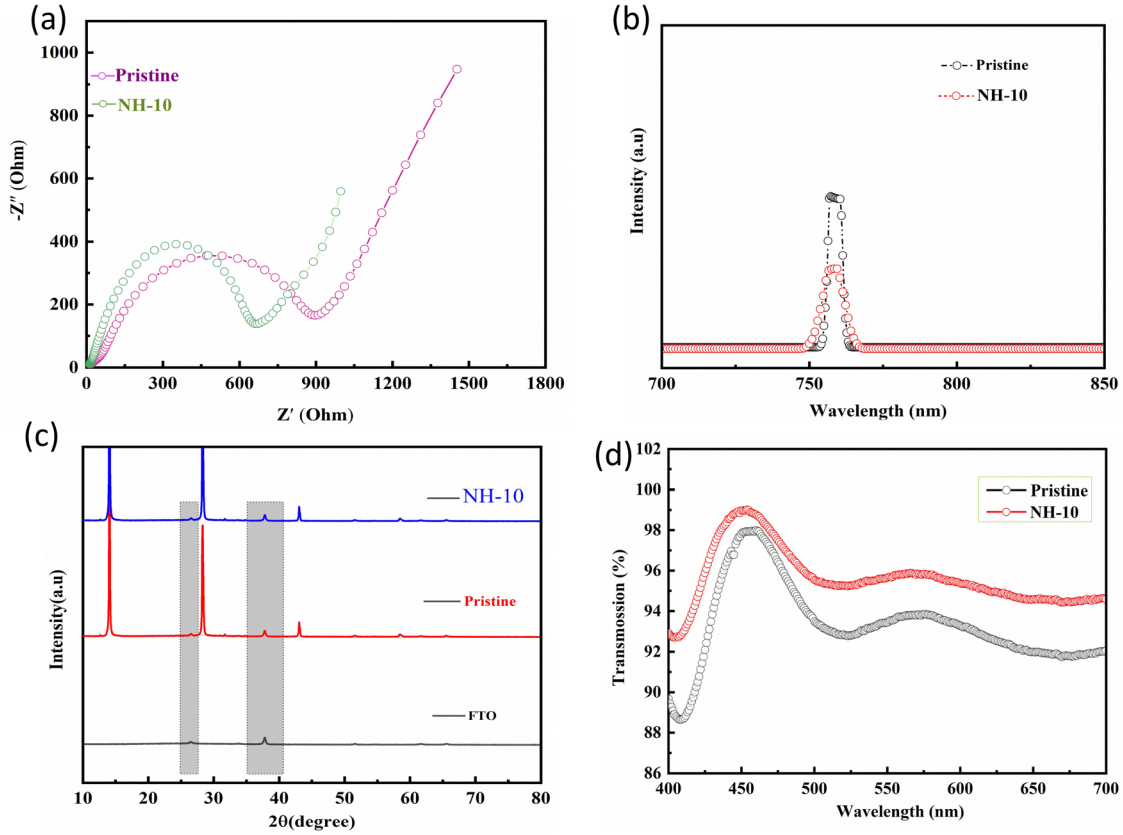

Fig. 4 Geometrical and optoelectronic properties analysis, (a) EIS spectra, (b) PL spectra of the perovskite layer on HTL/FTO, (c) XRD pattern of the perovskite layer deposited on FTO, and (d) transmittance spectra of the pristine PEDOT: PSS and NH_4Cl-10 doped PEDOT: PSS.

impedance peaks, an increase in the magnitude of the impedance, or a change in the shape of the impedance spectrum. This information can be used to further optimize the performance of the solar cell and to develop a better understanding of the underlying causes of the improvement in the Jsc value (Fig. 4a). In order to well study the steady state photoluminescence (PL) analyses and optical absorption spectra, we have assembled a half-cell structure containing FTO/PEDOT: PSS or NH_4Cl with various concentration doped-PEDOT: PSS/perovskite (Fig. S7, ESI†). The FTO/NH_4Cl-10 doped PEDOT: PSS/perovskite has a remarkable photovoltaic performance, much higher than pristine FTO/PEDOT: PSS (Fig. 4b). The optimized device displays a very noticeable (sharp) PL peak intensity at 761 nm compared with pristine PEDOT: PSS, which suggests higher radiative recombination. Such a stronger recombination indicates weaker nonradiative recombination. It is worth noting that the NH_4Cl-doped HTL plays a crucial role in hole extraction across perovskite HTL interfaces and charges fewer recombination centers, which improves the photovoltaic performance of NH_4Cl-10 doped PEDOT: PSS (HTL).[42] The crystal growth of the perovskite film fabricated on the surface of pristine and NH_4Cl doped PEDOT: PSS perovskite film was further investigated through X-ray diffraction (XRD) (Fig. 4c). The rough surface of the PEDOT: PSS film provides a high surface area for the growth of perovskite crystals, and the increased surface area can lead to an increased nucleation density. The increased nucleation density can result in the formation of more uniform and highly crystalline perovskite films, as the high surface area allows for the formation of a large number of nuclei, which grow into highly crystalline structures. Additionally, doping with NH_4Cl can help to stabilize the perovskite crystal structure by reducing the defects and dislocations in the material. This is because doping with NH_4Cl introduces positively charged impurities into the material, which help to balance the charges in the material and reduce the formation of defects and dislocations. The reduction in defects and dislocations results in an improvement in the overall crystallinity of the perovskite films and enhances their optoelectronic performance. Since, the highly crystalline materials have a more ordered and uniform structure, as a result improved charge transport and reduced recombination losses, leading to higher device performance. The XRD patterns for both pristine and NH_4Cl-10 doped PEDOT: PSS show the same diffraction peak of 14.13° and 28.41° with a corresponding plan symmetry of (110) and (220), respectively.[43,44] The NH_4Cl-10 doped PEDOT: PSS perovskite shows an intense peak with smaller full width at half maximum than that of pristine PEDOT: PSS perovskite films, which is attributed to the crystal growth along the (110) direction and improves the crystalline behavior of the perovskite layer.[45,46]

Transmittance properties were further analyzed to verify the enhanced photovoltaic properties of the NH_4Cl-10 doped

PEDOT: PSS. In the visible light range, the transmittance of NH_4Cl-10 PEDOT: PSS demonstrates better transmittance spectra than pristine PEDOT: PSS (Fig. 4d). The obtained pristine has a maximum transmittance in the 450 nm up to 98%, whereas NH_4Cl-10 doped PEDOT: PSS has achieved maximum transmittance up to 99.1%. In addition, the pristine PEDOT: PSS has obtained the transmittance after 500 nm to 650 nm region up to 92.5%, while the NH_4Cl-10 doped PEDOT: PSS has achieved 96.3%, respectively. The increased transmittance allows more sunlight capture and photon absorption *via* the active layer. On the other hand, the high concentration of NH_4Cl doped PEDOT: PSS causes decreased transmittance and adversely affects J_{sc} value, lowering the photovoltaic performance of PSCs.

In summary, we have demonstrated an innovative approach for improving the power conversion efficiency and surface roughness of inverted perovskite solar cells. NH_4Cl was successfully doped into a hole transporting layer PEDOT: PSS through spin coating. The optimized NH_4Cl-10 doped PEDOT: PSS HTL exhibits excellent photovoltaic performance with a higher J_{SC} value of 26.4, a FF of 79.7% and a V_{OC} of 1.02. Furthermore, compared to other NH_4Cl doped concentrations and pristine PEDOT: PSS, the optimized NH_4Cl-10 doped PEDOT: PSS HTL exhibits the highest conductivity, yielding a better PCE of 17.5%. NH_4Cl doped PEDOT: PSS HTL is believed to be an innovative, practical, and cost-effective method to achieve high conductivity and power conversion efficiency in PSCs.

Author contributions

S. Iqbal, S. Zaman and MB Hussain conceived the idea. S. Iqbal designed the experiments and performed the synthesis, physical characterization and electrochemical measurements. S. Iqbal and S. Zaman co-wrote and revised the manuscript. F. Zaman, R. Mehmood, AN. Chishti, A. Qayum, and S. Zaman participated in the scientific result discussions. All the authors contributed to the overall scientific interpretation.

Conflicts of interest

The authors declare no competing financial interests.

Acknowledgements

This work is supported by the by NSFC (51472110) and Shandong Provincial Natural Science Foundation (ZR2017ZB0316).

References

1 X. Sun, B. Zhang, M. Chen, L. Wang, D. Wang, R. Man, S. Iqbal, F. Tian, Y. Qian and L. Xu, Space-confined growth of Bi2Se3 nanosheets encapsulated in N-doped carbon shell lollipop-like composite for full/half potassium-ion and lithium-ion batteries, *Nano Today*, 2022, **43**, 101408.

2 S. Iqbal, L. Wang, Z. Kong, Y. Zhai, X. Sun, F. Wang, Z. Jing, X. He, J. Dou and L. Xu, In Situ Growth of CoS2/ZnS Nanoparticles on Graphene Sheets as an Ultralong Cycling Stability Anode for Potassium Ion Storage, *ACS Appl. Mater. Interfaces*, 2022, **14**, 15324–15336.

3 Z. Kong, L. Wang, S. Iqbal, B. Zhang, B. Wang, J. Dou, F. Wang, Y. Qian, M. Zhang and L. Xu, Iron Selenide-Based Heterojunction Construction and Defect Engineering for Fast Potassium/Sodium-Ion Storage, *Small*, 2022, **18**, 2107252.

4 S. Zaman, X. Tian, Y.-Q. Su, W. Cai, Y. Yan, R. Qi, A. I. Douka, S. Chen, B. You, H. Liu, S. Ding, X. Guo and B. Y. Xia, Direct integration of ultralow-platinum alloy into nanocarbon architectures for efficient oxygen reduction in fuel cells, *Sci. Bull.*, 2021, **66**, 2207–2216.

5 S. Zaman, M. Wang, H. Liu, F. Sun, Y. Yu, J. Shui, M. Chen and H. Wang, Carbon-based catalyst supports for oxygen reduction in proton-exchange membrane fuel cells, *Trends Chem.*, 2022, **4**, 886–906.

6 S. Chen, Z. Zhang, W. Jiang, S. Zhang, J. Zhu, L. Wang, H. Ou, S. Zaman, L. Tan, P. Zhu, E. Zhang, P. Jiang, Y. Su, D. Wang and Y. Li, Engineering Water Molecules Activation Center on Multisite Electrocatalysts for Enhanced CO2 Methanation, *J. Am. Chem. Soc.*, 2022, **144**, 12807–12815.

7 S. Zaman, Y. Q. Su, C. L. Dong, R. Qi, L. Huang, Y. Qin, Y. C. Huang, F. M. Li, B. You, W. Guo, Q. Li, S. Ding and B. Yu Xia, Scalable molten salt synthesis of platinum alloys planted in metal-nitrogen-graphene for efficient oxygen reduction, *Angew. Chem., Int. Ed.*, 2022, **61**, 202115835–202115843.

8 K. Kim, Z. Wu, J. Han, Y. Ma, S. Lee, S.-K. Jung, J.-W. Lee, H. Y. Woo and I. Jeon, Homogeneously Miscible Fullerene inducing Vertical Gradient in Perovskite Thin-Film toward Highly Efficient Solar Cells, *Adv. Energy Mater.*, 2022, **12**, 2200877.

9 J. Liu, N. Li, J. Jia, J. Dong, Z. Qiu, S. Iqbal and B. Cao, Perovskite films grown with green mixed anti-solvent for highly efficient solar cells with enhanced stability, *Sol. Energy*, 2019, **181**, 285–292.

10 Z. C. Lin, W. Q. Zhang, Q. B. Cai, X. N. Xu, H. Y. Dong, C. Mu and J. P. Zhang, Complexation Engineering of Electron Transport Layers for High-Performance Perovskite Solar Cells, *Sol. RRL*, 2022, **6**, e2200343.

11 L. Wang, Q. Song, F. Pei, Y. Chen, J. Dou, H. Wang, C. Shi, X. Zhang, R. Fan, W. Zhou, Z. Qiu, J. Kang, X. Wang, A. Lambertz, M. Sun, X. Niu, Y. Ma, C. Zhu, H. Zhou, J. Hong, Y. Bai, W. Duan, K. Ding and Q. Chen, Strain Modulation for Light-Stable n–i–p Perovskite/Silicon Tandem Solar Cells, *Adv. Mater.*, 2022, **34**, 2201315.

12 D. Zheng, C. Schwob, Y. Prado, Z. Ouzit, L. Coolen and T. Pauporté, How do gold nanoparticles boost the performance of perovskite solar cells?, *Nano Energy*, 2022, **94**, 106934.

13 H. K. Gong, Q. Song, C. Ji, H. M. Zhang, C. J. Liang, F. L. Sun, C. H. Zhang, A. Q. Yang, D. Li, X. P. Jing, F. T. You and Z. Q. He, Molecular interactions and functionalities of an organic additive in a perovskite semiconducting device: a case study

towards high performance solar cells, *J. Mater. Chem. A*, 2022, **10**, 2876–2887.

14 H. Gong, Q. Song, C. Ji, H. Zhang, C. Liang, F. Sun, C. Zhang, A. Yang, D. Li, X. Jing, F. You and Z. He, Molecular interactions and functionalities of an organic additive in a perovskite semiconducting device: a case study towards high performance solar cells, *J. Mater. Chem. A*, 2022, **10**, 2876–2887.

15 A. Shandilya, K. Schwarz and R. Sundararaman, Erratum: ''Interfacial water asymmetry at ideal electrochemical interfaces'' [J. Chem. Phys. 156, 014705 (2022)], *J. Chem. Phys.*, 2022, **156**, 129901.

16 S.-S. Li, C.-H. Chang, Y.-C. Wang, C.-W. Lin, D.-Y. Wang, J.-C. Lin, C.-C. Chen, H.-S. Sheu, H.-C. Chia, W.-R. Wu, U. S. Jeng, C.-T. Liang, R. Sankar, F.-C. Chou and C.-W. Chen, Intermixing-seeded growth for high-performance planar heterojunction perovskite solar cells assisted by precursor-capped nanoparticles, *Energy Environ. Sci.*, 2016, **9**, 1282–1289.

17 M.-H. Li, C.-W. Hsu, P.-S. Shen, H.-M. Cheng, Y. Chi, P. Chen and T.-F. Guo, Novel spiro-based hole transporting materials for efficient perovskite solar cells, *Chem. Commun.*, 2015, **51**, 15518–15521.

18 W. S. Yang, B. W. Park, E. H. Jung, N. J. Jeon, Y. C. Kim, D. U. Lee, S. S. Shin, J. Seo, E. K. Kim, J. H. Noh and S. I. Seok, Iodide management in formamidinium-lead-halide-based perovskite layers for efficient solar cells, *Science*, 2017, **356**, 1376–1379.

19 S. L. Zhang, M. Xu, C. Zhang, Y.-C. Wang, H. Zou, X. He, Z. Wang and Z. L. Wang, Rationally designed sea snake structure based triboelectric nanogenerators for effectively and efficiently harvesting ocean wave energy with minimized water screening effect, *Nano Energy*, 2018, **48**, 421–429.

20 L. Hu, M. Li, K. Yang, Z. Xiong, B. Yang, M. Wang, X. Tang, Z. Zang, X. Liu, B. Li, Z. Xiao, S. Lu, H. Gong, J. Ouyang and K. Sun, PEDOT:PSS monolayers to enhance the hole extraction and stability of perovskite solar cells, *J. Mater. Chem. A*, 2018, **6**, 16583–16589.

21 L. Hu, J. Fu, K. Yang, Z. Xiong, M. Wang, B. Yang, H. Wang, X. Tang, Z. Zang, M. Li, J. Li and K. Sun, Inhibition of In-Plane Charge Transport in Hole Transfer Layer to Achieve High Fill Factor for Inverted Planar Perovskite Solar Cells, *Sol. RRL*, 2019, **3**, 1900104.

22 C. Wang, K. Sun, J. Fu, R. Chen, M. Li, Z. Zang, X. Liu, B. Li, H. Gong and J. Ouyang, Enhancement of Conductivity and Thermoelectric Property of PEDOT:PSS via Acid Doping and Single Post-Treatment for Flexible Power Generator, *Adv. Sustainable Syst.*, 2018, **2**, 1800085.

23 L. Zhang, K. Yang, R. Chen, Y. Zhou, S. Chen, Y. Zheng, M. Li, C. Xu, X. Tang, Z. Zang and K. Sun, The Role of Mineral Acid Doping of PEDOT:PSS and Its Application in Organic Photovoltaics, *Adv. Electron. Mater.*, 2020, **6**, 1900648.

24 D.-X. Yuan, X.-D. Yuan, Q.-Y. Xu, M.-F. Xu, X.-B. Shi, Z.-K. Wang and L.-S. Liao, A solution-processed bathocuproine cathode interfacial layer for high-performance bromine–iodine perovskite solar cells, *Phys. Chem. Chem. Phys.*, 2015, **17**, 26653–26658.

25 E. D. Jung, A. K. Harit, D. H. Kim, C. H. Jang, J. H. Park, S. Cho, M. H. Song and H. Y. Woo, Multiply Charged Conjugated Polyelectrolytes as a Multifunctional Interlayer for Efficient and Scalable Perovskite Solar Cells, *Adv. Mater.*, 2020, **32**, 2002333.

26 X. Wan, Y. Jiang, Z. Qiu, H. Zhang, X. Zhu, I. Sikandar, X. Liu, X. Chen and B. Cao, Zinc as a New Dopant for NiOx-Based Planar Perovskite Solar Cells with Stable Efficiency near 20%, *ACS Appl. Energy Mater.*, 2018, **1**, 3947–3954.

27 B. Shi, J. Jia, X. Feng, G. Ma, Y. Wu and B. Cao, Thermal evaporated CuI film thickness-dependent performance of perovskite solar cells, *Vacuum*, 2021, **187**, 110076.

28 W. Sun, Y. Li, S. Ye, H. Rao, W. Yan, H. Peng, Y. Li, Z. Liu, S. Wang, Z. Chen, L. Xiao, Z. Bian and C. Huang, High-performance inverted planar heterojunction perovskite solar cells based on a solution-processed CuOx hole transport layer, *Nanoscale*, 2016, **8**, 10806–10813.

29 Y. Xia and J. Ouyang, PEDOT:PSS films with significantly enhanced conductivities induced by preferential solvation with cosolvents and their application in polymer photovoltaic cells, *J. Mater. Chem.*, 2011, **21**, 4927–4936.

30 X. Huang, R. Bäuerle, F. Scherz, J.-N. Tisserant, W. Kowalsky, R. Lovrinčić and G. Hernandez-Sosa, Improved performance of perovskite light-emitting diodes with a NaCl doped PEDOT:PSS hole transport layer, *J. Mater. Chem. C*, 2021, **9**, 4344–4350.

31 Z. Zhu, H. Song, J. Xu, C. Liu, Q. Jiang and H. Shi, Significant conductivity enhancement of PEDOT:PSS films treated with lithium salt solutions, *J. Mater. Sci.: Mater. Electron.*, 2015, **26**, 429–434.

32 J. Qiu, X. Xia, Z. Hu, S. Zhou, Y. Wang, Y. Wang, R. Zhang, J. Li and Y. Zhou, Molecular ammonia sensing of PEDOT:PSS/nitrogen doped MXene Ti3C2Tx composite film at room temperature, *Nanotechnology*, 2021, **33**, 065501.

33 J. Hossain, Q. Liu, T. Miura, K. Kasahara, D. Harada, R. Ishikawa, K. Ueno and H. Shirai, Nafion-Modified PEDOT:PSS as a Transparent Hole-Transporting Layer for High-Performance Crystalline-Si/Organic Heterojunction Solar Cells with Improved Light Soaking Stability, *ACS Appl. Mater. Interfaces*, 2016, **8**, 31926–31934.

34 O. A. Ghazy, M. M. Ibrahim, F. I. Abou Elfadl, H. M. Hosni, E. M. Shehata, N. M. Deghiedy and M. R. Balboul, PEDOT:PSS incorporated silver nanoparticles prepared by gamma radiation for the application in organic solar cells, *J. Radiat. Res. Appl. Sci.*, 2015, **8**, 166–172.

35 A. S. Pranti, A. Schander, A. Bödecker and W. Lang, PEDOT:PSS coating on gold microelectrodes with excellent stability and high charge injection capacity for chronic neural interfaces, *Sens. Actuators, B*, 2018, **275**, 382–393.

36 Y. Park, K. Soon Choi and S. Young Kim, Graphene oxide/PEDOT:PSS and reduced graphene oxide/PEDOT:PSS hole extraction layers in organic photovoltaic cells, *Phys. Status Solidi A*, 2012, **209**, 1363–1368.

37 R. M. Vedovatte, M. C. Saccardo, E. L. Costa and C. E. Cava, PEDOT:PSS post-treated by DMSO using spin coating, roll-to-roll and immersion: a comparative study, *J. Mater. Sci.: Mater. Electron.*, 2020, **31**, 317–323.
38 S. Zaman, L. Huang, A. I. Douka, H. Yang, B. You and B. Y. Xia, Oxygen reduction electrocatalysts toward practical fuel cells: progress and perspectives, *Angew. Chem., Int. Ed.*, 2021, **60**, 17832–17852.
39 P. Li, M. I. Omer Mohamed, C. Xu, X. Wang and X. Tang, Electrical property modified hole transport layer (PEDOT:PSS) enhance the efficiency of perovskite solar cells: Hybrid co-solvent post-treatment, *Org. Electron.*, 2020, **78**, 105582.
40 L. Hu, K. Sun, M. Wang, W. Chen, B. Yang, J. Fu, Z. Xiong, X. Li, X. Tang, Z. Zang, S. Zhang, L. Sun and M. Li, Inverted Planar Perovskite Solar Cells with a High Fill Factor and Negligible Hysteresis by the Dual Effect of NaCl-Doped PEDOT:PSS, *ACS Appl. Mater. Interfaces*, 2017, **9**, 43902–43909.
41 F. X. Xie, W. C. H. Choy, C. C. D. Wang, W. E. I. Sha and D. D. S. Fung, Improving the efficiency of polymer solar cells by incorporating gold nanoparticles into all polymer layers, *Appl. Phys. Lett.*, 2011, **99**, 153304.
42 K. Yang, S. Chen, J. Fu, S. Jung, J. Ye, Z. Kan, C. Hu, C. Yang, Z. Xiao, S. Lu and K. Sun, Molecular Lock Induced by Chloroplatinic Acid Doping of PEDOT:PSS for High-Performance Organic Photovoltaics, *ACS Appl. Mater. Interfaces*, 2020, **12**, 30954–30961.
43 W. Sun, Y. Li, Y. Xiao, Z. Zhao, S. Ye, H. Rao, H. Ting, Z. Bian, L. Xiao, C. Huang and Z. Chen, An ammonia modified PEDOT: PSS for interfacial engineering in inverted planar perovskite solar cells, *Org. Electron.*, 2017, **46**, 22–27.
44 F. M. Li, L. Huang, S. Zaman, W. Guo, H. Liu, X. Guo and B. Y. Xia, Corrosion Chemistry of Electrocatalysts, *Adv. Mater.*, 2022, **34**, e2200840.
45 A. Gautam and F. C. J. M. van Veggel, Synthesis of InN@SiO2 Nanostructures and Fabrication of Blue LED Devices, *ACS Appl. Mater. Interfaces*, 2012, **4**, 3902–3909.
46 S. Zaman, A. I. Douka, L. Noureen, X. Tian, Z. Ajmal and H. Wang, Oxygen reduction performance measurements: Discrepancies against benchmarks, *Battery Energy*, 2023, **1**, 20220060.

